

Normal and anomalous scaling of turbulence

J. Qian

Department of Physics, Graduate School of Academia Sinica, P.O. Box 3908, Beijing 100039, China

(Received 15 October 1997; revised manuscript received 3 June 1998)

A non-Gaussian model of the probability density function (PDF) of $|\Delta u_r|$ is proposed to study how the scaling exponents S_p of the structure function $\langle |\Delta u_r|^p \rangle$ of finite Reynolds number turbulence depends upon the Taylor-microscale Reynolds number R_λ . Here Δu_r is the longitudinal velocity difference across a distance r , and $\langle \rangle$ is the statistical average. The model not only predicts anomalous scaling ($S_p < p/3$ for $p > 3$) observed in experiments at a finite Reynolds number, but also predicts that S_p approaches normal scaling $p/3$ while R_λ is very high. Hence, in contrast to the prevailing multiscaling models, the non-Gaussian PDF model suggests a completely different picture of scaling of isotropic turbulence: the anomalous scaling observed in experiments is a finite Reynolds number effect, and the normal scaling is valid in the real Kolmogorov inertial range corresponding to an infinite Reynolds number.

[S1063-651X(98)03312-1]

PACS number(s): 47.27.Gs, 47.27.Jv

The issue of normal and anomalous scaling of isotropic turbulence is a hot topic of statistical physics of turbulence [1]. The structure function of order p is defined as $\langle |\Delta u_r|^p \rangle$ or $\langle \Delta u_r^p \rangle$, where $\langle \rangle$ is the statistical average and Δu_r is the longitudinal velocity difference across a distance r . In the inertial range, $\langle |\Delta u_r|^p \rangle \sim r^{\zeta_p}$ or $\langle \Delta u_r^p \rangle \sim r^{\zeta_p}$, and ζ_p is the scaling exponent of order p . Strictly speaking, ζ_p is defined for the idealized model of inertial range corresponding to the asymptotic case of an infinite Reynolds number, and is called the real (or theoretical) inertial range scaling exponent in this paper. According to Kolmogorov's theory of 1941 (K41) [2], $\zeta_p = p/3$ (normal scaling). However, the experimental values of high-order scaling exponents are substantially lower than the K41 prediction [3,4]. In order to explain this anomalous scaling observed in experiments, various intermittency models have been developed [1]. We have shown [5] that the scaling range found in experiments is not the same as the real Kolmogorov inertial range, and the finite Reynolds number effect should be considered in comparing experiments with theories of inertial-range statistics. In fact, the structure functions do not exactly follow power laws over the (approximate) scaling range found in experiments, which is commonly called inertial range in the literature and actually is not the real Kolmogorov inertial range [5]. The quality of the power-law behavior is modest even at a large Reynolds number, and a curvature of the structure functions is generally visible on a log-log plot [6]. Therefore, in order to solve the issue of normal and anomalous scaling of isotropic turbulence, it is indispensable to study whether and how the scaling exponents obtained by experiments at a finite Reynolds number differ from the real inertial-range scaling exponent ζ_p at an infinite Reynolds number. In this paper, a non-Gaussian model of probability density function (PDF) of $|\Delta u_r|$ is proposed to study how the scaling exponents S_p of $\langle |\Delta u_r|^p \rangle$ of a finite Reynolds number turbulence depend upon the Taylor-microscale Reynolds number R_λ . The non-Gaussian PDF model not only predicts anomalous scaling ($S_p < p/3$ for $p > 3$) observed in experiments at a finite Reynolds number, but also predicts that S_p approaches normal scaling $p/3$ while $R_\lambda \rightarrow \infty$. Hence, in contrast to the prevail-

ing multiscaling models, the non-Gaussian PDF model suggests a completely different picture of scaling of isotropic turbulence: the anomalous scaling observed in experiments is a finite Reynolds number effect, and the normal scaling is valid in the real Kolmogorov inertial range at an infinite Reynolds number. First we explain how this conclusion is obtained, and then discuss its implication and relevant issues.

Let $P(x)$ be the PDF of $x = |\Delta u_r|/D_{LL}(r)^{1/2}$, where $D_{LL}(r) = \langle \Delta u_r^2 \rangle$ is the second-order structure function. We have

$$\langle |\Delta u_r|^p \rangle = D_{LL}(r)^{p/2} \langle x^p \rangle, \quad \langle x^p \rangle = \int_0^\infty x^p P(x) dx. \quad (1)$$

Although we are not able to derive the expression of $P(x)$ from the Navier-Stokes equations, the experimental data of PDF of Δu_r can be used to derive the form of $P(x)$. According to the experimental data [7], we have

$$P(x) = P_0 \exp(-Bx^\mu) \quad \text{while } x > 2 \quad (2)$$

and the parameters P_0 , B , and μ are functions of r . Reference [7] discussed the question of over what r range Eq. (2) is valid. For the study of scaling exponents S_p , it is enough to know that Eq. (2) is valid over the (approximate) scaling range.

The PDF of the absolute value of a Gaussian random variable is

$$P_G(x) = (2/\pi)^{1/2} \exp(-x^2/2), \quad 0 \leq x < \infty. \quad (3)$$

By the definition of $P(x)$ and $P_G(x)$, we have

$$\int_0^\infty P(x) dx = \int_0^\infty P_G(x) dx = 1 \quad (4)$$

and

$$\int_0^\infty x^2 P(x) dx = \int_0^\infty x^2 P_G(x) dx = 1. \quad (5)$$

Therefore, $P(x)$ and $P_G(x)$ intersect at two points x_1 and x_2 , i.e.,

TABLE I. Dependence of S_p upon boundary condition (BC), d , μ_m , K , and n for the case of $R_\lambda = 800$ and $C_D = 0.75$. K is the Kolmogorov constant.

BC	d	μ_m	K	n	S_2	S_4	S_6	S_8	S_{10}	S_{12}
(8a)	2.6	1.0	1.2	2	0.694	1.28	1.78	2.21	2.57	2.89
(8b)	2.6	1.0	1.2	2	0.694	1.28	1.78	2.21	2.58	2.91
(8c)	2.6	1.0	1.2	2	0.694	1.28	1.78	2.21	2.58	2.90
(8a)	2.6	1.0	1.5	2	0.693	1.28	1.79	2.22	2.59	2.92
(8b)	2.6	1.0	1.5	2	0.693	1.28	1.79	2.22	2.60	2.94
(8c)	2.6	1.0	1.5	2	0.693	1.28	1.79	2.22	2.60	2.93
(8a)	2.556	1.0	1.2	2	0.694	1.28	1.79	2.24	2.63	2.98
(8a)	2.667	1.0	1.2	2	0.694	1.28	1.76	2.16	2.48	2.75
(8a)	2.6	0.8	1.2	2	0.694	1.28	1.78	2.21	2.59	2.93
(8a)	2.6	1.2	1.2	2	0.694	1.28	1.78	2.20	2.56	2.88
(8b)	2.6	0.8	1.2	2	0.694	1.28	1.78	2.22	2.61	2.95
(8b)	2.6	1.2	1.2	2	0.694	1.28	1.78	2.21	2.57	2.89
(8a)	2.6	1.0	1.2	1	0.697	1.28	1.75	2.15	2.48	2.76
(8a)	2.6	1.0	1.2	4	0.692	1.29	1.80	2.24	2.63	2.97
(8c)	2.6	1.0	1.2	1	0.697	1.28	1.75	2.15	2.49	2.77
(8c)	2.6	1.0	1.2	4	0.692	1.29	1.80	2.24	2.63	2.98

$$P(x_1) = P_G(x_1) \quad \text{and} \quad P(x_2) = P_G(x_2). \quad (6)$$

According to the experimental data of Tabeling *et al.* [7], x_1 is around 0.5 and x_2 is around 2.4 (this author thanks Professor Tabeling for providing enlarged Figures of their experimental data). In the scaling range, a simple and reasonable representation of $P(x)$ is

$$P(x) = \exp[-f(x)], \quad (7a)$$

$$f(x) = -\ln(P_0) + Bx^\mu \quad \text{if } x \geq x_2, \quad (7b)$$

$$f(x) = A_0 + A_1x + A_2x^2 + A_3x^3 \quad \text{if } x_1 \leq x \leq x_2, \quad (7c)$$

$$f(x) = B_0 + B_1x + B_2x^2 + B_3x^3 \quad \text{if } 0 \leq x \leq x_1. \quad (7d)$$

$P(x)$ and $f(x)$ are supposed to be continuous and smooth at x_1 and x_2 . Following the cubic spline method of applied mathematics, the coefficients A_i and B_i ($i=0,1,2,3$) in Eqs. (7c) and (7d) are determined by Eq. (6) and some boundary condition at $x=0$. Various boundary conditions (BC's) at $x=0$ have been used and compared. Table I shows the results for the following three typical cases:

$$B_3 = 0 \quad \text{and no BC at } x=0, \quad (8a)$$

$$df(x)/dx = 0 \quad \text{at } x=0, \quad (8b)$$

$$f(0) \text{ is given by some empirical formula.} \quad (8c)$$

By using experimental data of Tabeling *et al.* [7], it is easy to determine how $f(0)$ and μ change with r , and the empirical formula of Eq. (8c) can be obtained by a low-order polynomial fit. As shown in Table I, different boundary conditions at $x=0$ generate nearly the same high-order scaling exponents, although they lead to different behavior of $P(x)$ at small x . By Eqs. (3), (6), (7a), and (7b), we have

$$P_0 = (2/\pi)^{1/2} \exp(Bx_2^\mu - x_2^2/2). \quad (9)$$

Therefore, the PDF models (7) have four undetermined parameters B , μ , x_1 , and x_2 only; other parameters P_0 , A_i , and B_i ($i=0,1,2,3$) can be expressed in terms of B , μ , x_1 , and x_2 , so four independent conditions are needed to determine the PDF models (7) completely. We already have two conditions (4) and (5), and two other conditions are derived in the next paragraph. The parameter x_2 determined by the four conditions is between 2.3 and 2.5, while r is in the (approximate) scaling range. Since $x_2 > 2$, Eq. (7b) is just the experimental result (2).

If there is a scaling range for the structure functions $\langle |\Delta u_r|^p \rangle$ of isotropic turbulence, then in the scaling range we have

$$\langle x^4 \rangle / \langle x^3 \rangle^d = \text{const}, \quad (10)$$

where $\langle x^4 \rangle$ is the flatness, $\langle x^3 \rangle$ is the skewness, and the experimental value of the exponent d is around 2.6. Different intermittency models give different values of d , for example the log-normal model [8] gives $d=8/3$, the multifractal p model [9] gives $d=2.595$, and the She-Leveque model [10] leads to $d=2.556$. In our numerical calculation, these different values of d are used and compared, and the result is given in Table I. Different values of the constant of Eq. (10), which are compatible with the experimental data of Tabeling *et al.* [7], are also used and compared; they lead to nearly the same scaling exponents. In this paper, we deal with the structure functions $\langle |\Delta u_r|^p \rangle$ of the absolute value of Δu_r . According to Kolmogorov's similarity hypothesis, which underlies both K41 and K62 theory [2,8], $\langle |\Delta u_r|^p \rangle$ and $\langle \Delta u_r^p \rangle$ have the same scaling exponents. Of course, it is a controversial issue whether it is valid for odd p . In the case of $p=3$, experiments [11] show that $\langle |\Delta u_r|^3 \rangle$ and $D_{LLL}(r) = \langle \Delta u_r^3 \rangle$ have almost the same scaling exponent. Hence, in the scaling range, we have

$$\langle |\Delta u_r|^3 \rangle / D_{LLL}(r) = \text{const}. \quad (11)$$

Equations (4), (5), (10), and (11) are the four independent conditions to determine the four undetermined parameters B ,

μ , x_1 , and x_2 of the PDF models (7). The experimental values of the constant of Eq. (11) is around -5 to -4 ; its different values are used in our numerical calculation and give nearly the same scaling exponents.

Now we outline how to apply the above non-Gaussian PDF model to calculate the scaling exponents S_p of $\langle |\Delta u_r|^p \rangle$ of finite Reynolds number turbulence. First of all, we have to determine the r dependence of the four undetermined parameters B , μ , x_1 , and x_2 of the PDF models (7). In order to use Eqs. (4), (5), (10), and (11) to determine the r dependence of the parameters B , μ , x_1 , and x_2 , the second-order structure function $D_{LL}(r)$ and the third-order structure function $D_{LLL}(r)$ are needed. For given R_λ , by using the procedure described in Ref. [5], we calculate the third-order structure function $D_{LLL}(r)$. The three-dimensional energy spectrum is

$$E(k) = K\varepsilon^{2/3}k^{-5/3}F(k/k_d)/[1 + (k_0/k)^{n+5/3}], \quad (12)$$

and $F(k/k_d)$ is obtained by solving the spectral dynamic equation numerically [5]. Here K is the Kolmogorov constant, ε is energy dissipation rate, $k_d = (\varepsilon/\nu^3)^{1/4}$ is the Kolmogorov wave number, ν is the kinematic viscosity, and k_0 and n are large-scale parameters. Different values of K and n are used in our numerical calculation to see their effect on S_p , which is shown in Table I. By using Eq. (12) and

$$D_{LL}(r) = 4 \int_0^\infty E(k) [1/3 + \cos(kr)/(kr)^2 - \sin(kr)/(kr)^3] dk, \quad (13)$$

we obtain the second-order structure function $D_{LL}(r)$ (Moin and Yaglom [1]). The resultant $D_{LLL}(r)$ and $D_{LL}(r)$ are checked: in the universal equilibrium range $D_{LLL}(r)$ and $D_{LL}(r)$ should satisfy the Kolmogorov equation, which is an exact statistical result of the Navier-Stokes equation [1], and $D_{LL}(r)$ should be compatible with Batchelor's formula, which fits the experimental data of $D_{LL}(r)$ very well. After $D_{LL}(r)$ and $D_{LLL}(r)$ are derived and checked, Eqs. (4), (5), (10), and (11) are used to determine how the four undetermined parameters B , μ , x_1 , and x_2 of the PDF models (7) change with r in the (approximate) scaling range for a given R_λ ; as mentioned above, other parameters P_0 , A_i , and B_i of the models (7) are expressed in terms of B , μ , x_1 , and x_2 . By using Eqs. (1) and (7), we calculate how $\langle |\Delta u_r|^p \rangle$ changes with r in the scaling range for a given R_λ . Finally, within the scaling range, the log-log plot of $\langle |\Delta u_r|^p \rangle$ against r is fitted by a straight line using the least-squares method, and its slope is the scaling exponents S_p . The result is given in Fig. 1, and the meaning of C_D and μ_m is explained in the next paragraph.

Before discussing our results, it is necessary to explain how to determine the scaling range $r_1 \leq r \leq r_2$ of finite Reynolds number turbulence. We use $D_{LLL}(r)$ to determine the scaling range. From the Navier-Stokes equations, we have [1]

$$D_{LLL}(r) = -\left(\frac{4}{5}\right)\varepsilon r + \Psi + \Phi, \quad \Psi = 6\nu dD_{LL}(r)/dr, \quad (14)$$

where Φ is a term representing the effect of large-scale motion. According to Kolmogorov [2,8], the inertial range is the

small-scale range within which the terms Ψ and Φ on the right-hand side of Eq. (14) are negligible, so

$$D_{LLL}(r) = -\left(\frac{4}{5}\right)\varepsilon r \quad \text{or} \quad -D_{LLL}(r)/\varepsilon r = 0.8, \quad (15)$$

which is the celebrated Kolmogorov $\frac{4}{5}$ law. Since the terms Ψ and Φ of Eq. (14) approach zero algebraically and very slowly, strictly speaking, the power law (15) is valid only for the asymptotic case of an infinite Reynolds number. As shown in [5], within the scaling range found in experiments at a finite Reynolds number, $-D_{LLL}(r)/\varepsilon r$ is substantially lower than 0.8, and is not a constant independent of r (see Fig. 1 of Ref. [5]), so the scaling $D_{LLL} \sim r$ is not exact. The scaling range is called ‘‘inertial range’’ in the literature, but actually is not the real Kolmogorov inertial range [5]. Obviously the (approximate) scaling range is around the maximum point r_m , where $-D_{LLL}(r)/\varepsilon r$ takes its maximum value and changes with r slowly around r_m . The scaling exponent S_3 of $D_{LLL}(r)$ over $r_1 \leq r \leq r_2$ is calculated by the least-squares method mentioned above (S_3 is a special case of S_p for $p=3$), and its value changes as the r range $r_1 \leq r \leq r_2$ changes. As a common practice, it is required that the scaling exponent S_3 over $r_1 \leq r \leq r_2$ is equal to 1. The scaling exponent S_3 over the range $r_1 \leq r \leq r_2$ is a function of r_1 and r_2 , denoted by $S_3(r_1, r_2)$. Generally speaking, there are many (r_1, r_2) satisfying $S_3(r_1, r_2) = 1$ when the range $r_1 \leq r \leq r_2$ is around r_m . Hence there are many r ranges around r_m over which $S_3 = 1$. In our calculation, the scaling range $r_1 \leq r \leq r_2$ is defined as the widest r range satisfying the following conditions:

$$\text{Scaling exponent } S_3 \text{ of } D_{LLL}(r) \text{ over } r_1 \leq r \leq r_2 = 1, \quad (16a)$$

$$-D_{LLL}(r)/\varepsilon r \geq C_D \quad \text{when } r_1 \leq r \leq r_2, \quad C_D < 0.8. \quad (16b)$$

According to [5], if $C_D = 0.795$, there is no scaling range while $R_\lambda < 5000$. If $C_D = 0.7$, there is a scaling range of nearly two decades for $R_\lambda = 2000$, and the quality of the power-law behavior is modest over the scaling range; the larger C_D is, the narrower the scaling range $r_1 \leq r \leq r_2$ becomes, and the better is the quality of the power-law behavior in the scaling range. As C_D approaches 0.8, the critical R_λ for the existence of the scaling range $r_1 \leq r \leq r_2$ becomes higher and higher, and the scaling range approaches the real inertial range. Hence, we have

$$S_p \rightarrow \zeta_p \quad \text{as } C_D \rightarrow 0.8 \text{ and } R_\lambda \rightarrow \infty, \quad (17)$$

where ζ_p is the real (or theoretical) inertial range scaling exponents. The factor μ_m in Table I and Figs. 1 and 2 is the value of μ of Eq. (7b) at $r = r_m$, and different values of μ_m correspond to different values of the constant of Eq. (11).

Figure 1 shows how the scaling exponents S_p of finite Reynolds number turbulence depend upon C_D and R_λ . The continuous line is for the case of $C_D = 0.795$, the small black squares are for $C_D = 0.75$, and the circles are for $C_D = 0.7$. In the case of $C_D = 0.795$, there is no scaling range $r_1 \leq r \leq r_2$ for $R_\lambda < 5000$. Over the scaling range $r_1 \leq r \leq r_2$, the quality of the power-law behavior $\langle |\Delta u_r|^p \rangle \sim r^{S_p}$ is modest for $C_D = 0.7$ and is improved as C_D increases. Table I shows how

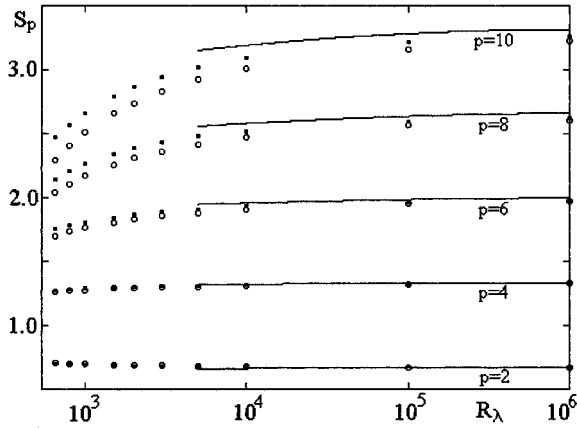


FIG. 1. The dependence of scaling exponent S_p upon C_D and R_λ for $p=2, 4, 6, 8,$ and 10 ; —, $C_D=0.795$; ■ ■ ■, $C_D=0.75$; ○ ○ ○, $C_D=0.7$; $K=1.2, n=2, d=2.6, \mu_m=1$, and the boundary condition is (8a) or (8b) or (8c).

the boundary condition (BC) and the factors $d, \mu_m, K,$ and n influence S_p for the case of $R_\lambda=800$ and $C_D=0.75$; the higher R_λ is, the smaller the influence will be. The S_p shown in Table I is in agreement with the famous experimental data of Anselmet *et al.* [3]. For all these $d, \mu_m, K, n,$ and the boundary conditions listed in Table I, the scaling exponents S_p approaches $p/3$ while $C_D \rightarrow 0.8$ and $R_\lambda \rightarrow \infty$.

According to Ref. [6], it is better to use the relative scaling exponents ζ_p^* of $\langle |\Delta u_r|^p \rangle$ against $\langle |\Delta u_r|^3 \rangle$ over the range $20 \leq r/\eta \leq 300$ to make a comparison with experiments in various flow configurations by the extended self-similarity method of Benzi *et al.* [11]; here $\eta=1/k_d$ is the Kolmogorov scale. In the framework of isotropic turbulence adopted in this paper, only two large-scale parameters k_0 and n of Eq. (12) are available to simulate the features of large-scale motion, and different k_0/k_d corresponds to different R_λ . Of course, the effect of large-scale shear motion cannot be considered in the framework of isotropic turbulence. The non-Gaussian PDF models (7) are used to calculate the relative scaling exponents ζ_p^* of $\langle |\Delta u_r|^p \rangle$ against $\langle |\Delta u_r|^3 \rangle$ over the range $20 \leq r/\eta \leq 300$ for p from 2 to 10, and the result is shown in Fig. 2, which is in agreement with the experimental data summarized in Fig. 3 of Ref. [6]. Therefore, Figs. 1 and

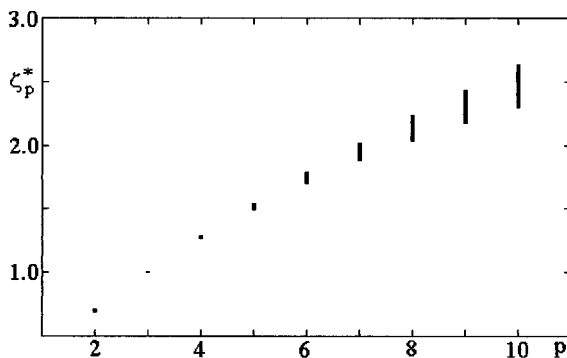


FIG. 2. The relative scaling exponents ζ_p^* of $\langle |\Delta u_r|^p \rangle$ against $\langle |\Delta u_r|^3 \rangle$ for various values of large-scale parameters n and k_0 ($n=1, 2,$ and 4 ; the range of k_0/k_d corresponds to $800 \leq R_\lambda \leq 10^4$). $K=1.2, d=2.6, \mu_m=1$, and the boundary condition is (8a) or (8b) or (8c).

2 clearly show that the non-Gaussian PDF model not only predicts (absolute and relative) anomalous scaling observed in experiments at a finite Reynolds number, but also predicts that S_p approaches normal scaling $p/3$ while $R_\lambda \rightarrow \infty$, so the anomalous scaling observed in experiments is a finite Reynolds number effect. It should be mentioned that Grossmann *et al.* and Vainshtein and Sreenivasan [12] have studied the issue of the finite Reynolds number effect on the scaling exponents from different viewpoints.

An important issue is whether the available data deny K41 normal scaling ($\zeta_p=p/3$). Kadanoff [13] pointed out that, “Theory cannot for the moment distinguish the weak fluctuation of K41 and the intermittency of K62. To settle a question of this kind we should look to experiments. The experimental evidence suggests the existence of intermittency but is not yet conclusive.” In fact, the available experimental data do not deny asymptotic K41 scaling of isotropic turbulence if the data are properly interpreted. The (approximate) scaling range found in experiments at a finite Reynolds number is not the real Kolmogorov inertial range of isotropic turbulence [5]. The experimental structure functions do not clearly exhibit power law even at a large Reynolds number (on a log-log plot a curvature of the structure function is visible in the scaling range) [6]. In some flow configurations such as geophysical flows, due to the strong shearing effect, the (approximate) scaling range cannot be described by an isotropic turbulence models. Kraichnan [14] said, “relatively little attention has been devoted to the prediction of turbulence statistics at finite Reynolds number . . . It is likely that the question of intermittency corrections to K41 can be resolved only when a detailed understanding of the dynamics at finite Reynolds numbers has been achieved.” Moreover, in some cases, the so-called experimental evidence of K62 scaling actually favors K41 normal scaling if the data are properly interpreted. For example, by using the Kolmogorov equation, we [15] have shown that the experimental and numerical results of the second-order relative scaling exponent being 0.7 (which was previously interpreted as a clear evidence of K62 scaling) actually favors K41 scaling ($\zeta_2=2/3$) rather than K62 scaling ($\zeta_2=0.7$). In this paper, we demonstrate that the anomalous scaling ($S_p < p/3$ and $\zeta_p^* < p/3$ while $p > 3$) found in experiments at a finite Reynolds number is compatible with the K41 normal scaling ($\zeta_p=p/3$), because both of them are logical consequences of the same non-Gaussian PDF model.

Finally we make a summary. The PDF models (7) with the four conditions (4), (5), (10), and (11) are a simple and reasonable expression of experimental facts, and μ of Eq. (7b) is much lower than 2 in the scaling range, so the model is highly non-Gaussian. The non-Gaussian model not only predicts anomalous scaling observed in experiments at a finite Reynolds number, but also predicts that the real (or theoretical) inertial-range scaling exponent ζ_p is $p/3$, which is the limit value of S_p as $C_D \rightarrow 0.8$ and $R_\lambda \rightarrow \infty$. As shown in Fig. 1, the higher the order p is, the slower is S_p approaching $\zeta_p=p/3$; hence, in the experimental range of R_λ , the higher the order p is, the larger will be the deviation of S_p from $\zeta_p=p/3$. In contrast to the prevailing multiscaling models, our results suggest a completely different picture of scaling of isotropic turbulence: the anomalous scaling observed in experiments is a finite Reynolds number effect, and the nor-

mal scaling ($\zeta_p = p/3$) is valid in the real Kolmogorov inertial range corresponding to an infinite Reynolds number. One issue is whether the asymptotic K41 behavior is just a consequence of the particular fitting form of Eqs. (7a)–(7d) for $P(x)$. Several different fitting forms for $P(x)$ have been tested (see the Appendix), the asymptotic behavior remains the same as long as the well-grounded conditions (2), (4), (5), (10), and (11) are satisfied, and the same $D_{LLL}(r)$ and $D_{LL}(r)$ are used. For understanding our results, it is essential to realize that the finite Reynolds number effect decreases algebraically and slowly as $R_\lambda \rightarrow \infty$; the (approximate) scaling range found in experiments at a finite Reynolds number is not the real Kolmogorov inertial range. In comparing experiments with theories of inertial-range statistics, the finite Reynolds number effect should be considered. The absolute or relative scaling exponents S_p or ζ_p^* found in experiments at a finite Reynolds number are not the same as the real inertial-range scaling exponent ζ_p . The anomalous scaling ($S_p < p/3$ and $\zeta_p^* < p/3$ while $p > 3$) found in experiments at a finite Reynolds number is compatible with K41 normal scaling ($\zeta_p = p/3$).

This work was supported by the Natural Science Foundation of China and the Research Program ‘‘Non-linear Science.’’

APPENDIX: FITTING FORMS FOR $P(x)$

We describe the fitting forms of $P(x)$ which have been tested. Let $f(x) = -\ln(P(x))$, where $f(x)$ changes with x much slower than $P(x)$. Since $P(x)$ should be in conformity with the experimental fact (2), we have Eq. (7b), so we only need to fit $P(x)$ or $f(x)$ over the interval $0 \leq x \leq x_2$. $P(x)$ and the Gaussian PDF intersect at x_1 and x_2 , and $x_1 < x_2$. In order to reduce the fitting error, we divide the interval $0 \leq x \leq x_2$ into two smaller subintervals, i.e., $0 \leq x \leq x_1$ and $x_1 \leq x \leq x_2$.

The fitting forms over the interval $x_1 \leq x \leq x_2$ we have tested are

$$f(x) = A_0 + A_1x + A_2x^2 \quad \text{if } x_1 \leq x \leq x_2, \quad (\text{A1})$$

$$f(x) = A_0 + A_1x + A_2x^2 + A_3x^3 \quad \text{if } x_1 \leq x \leq x_2, \quad (\text{A2})$$

$$f(x) = A_0 + A_1x + A_2x^2 + A_3x^3 + A_4x^4 \quad \text{if } x_1 \leq x \leq x_2. \quad (\text{A3})$$

The fitting forms over the interval $0 \leq x \leq x_1$ we have tested are

$$f(x) = B_0 + B_1x^\beta \quad \text{if } 0 \leq x \leq x_1, \quad (\text{A4})$$

$$f(x) = B_0 + B_1x + B_2x^2 \quad \text{if } 0 \leq x \leq x_1, \quad (\text{A5})$$

$$f(x) = B_0 + B_1x + B_2x^2 + B_3x^3 \quad \text{if } 0 \leq x \leq x_1. \quad (\text{A6})$$

Three types of boundary conditions at $x=0$ are used, that is namely Eqs. (8a)–(8c). Different combinations of Eqs. (A1)–(A3), Eqs. (A4)–(A6) and Eqs. (8a)–(8c) yield many different fitting forms. The coefficients A_i , B_i , and β in Eqs. (A1)–(A3) and Eqs. (A4)–(A6) are determined by Eq. (6), proper continuity-smoothness conditions at x_1 and x_2 , and some boundary condition at $x=0$. The coefficients A_i , B_i , and β are expressed in terms of B , μ , x_1 , and x_2 . For example, the continuity-smoothness condition for Eqs. (A1) and (A4) is that $f(x)$ and $df(x)/dx$ are continuous at x_1 and x_2 , and the continuity-smoothness condition for Eqs. (A2) and (A6) is that $f(x)$, $df(x)/dx$, and $d^2f(x)/dx^2$ are continuous at x_1 and x_2 . The fitting form (7) corresponds to Eqs. (A2) and (A6) while using Eq. (8b) or Eq. (8c), and corresponds to Eqs. (A2) and (A5) while using Eq. (8a). According to our calculation, x_2 is between 2.3 and 2.5 and x_1 is around 0.5 while r is in the scaling range, hence $0 \leq x \leq x_1$ and $x_1 \leq x \leq x_2$ are quite narrow. Since $f(x)$ changes with x smoothly and slowly, it is reasonable to use a low-order polynomial or power function to express $f(x)$ over the narrow intervals $0 \leq x \leq x_1$ and $x_1 \leq x \leq x_2$. This is confirmed by our numerical calculation. It should be emphasized that all fitting forms of $f(x)$ have to satisfy the experimental fact (7b) for large x ($x > x_2$), and they are different only for small x ($x < x_2$). For the calculation of high-order structure functions, the behavior of $P(x)$ at large x is more important than its behavior at small x .

-
- [1] A. S. Monin and A. M. Yaglom, *Statistical Fluid Mechanics* (Cambridge University Press, Cambridge, 1975); M. Nelkin, *Adv. Phys.* **43**, 143 (1994); U. Frisch, *Turbulence: The Legacy of A. N. Kolmogorov* (Cambridge University Press, Cambridge, 1995).
- [2] A. N. Kolmogorov, *C. R. Acad. Sci. URSS* **30**, 301 (1941).
- [3] F. Anselmetti, Y. Gagne, E. J. Hopfinger, and R. A. Antonia, *J. Fluid Mech.* **140**, 63 (1984).
- [4] K. R. Sreenivasan and R. A. Antonia, *Annu. Rev. Fluid Mech.* **29**, 435 (1997).
- [5] J. Qian, *Phys. Rev. E* **55**, 337 (1997).
- [6] A. Arneodo *et al.*, *Europhys. Lett.* **34**, 411 (1996).
- [7] P. Tabeling, G. Zocchi, F. Belin, J. Maurer, and H. Willaume, *Phys. Rev. E* **53**, 1613 (1996); P. Kailasnath, K. R. Sreenivasan, and G. Stolovitzky, *Phys. Rev. Lett.* **68**, 2766 (1993); B. Castaing, Y. Gagne, and E. Hopfinger, *Physica D* **46**, 177 (1990).
- [8] A. N. Kolmogorov, *J. Fluid Mech.* **13**, 82 (1962).
- [9] C. Meneveau and K. R. Sreenivasan, *Phys. Rev. Lett.* **59**, 1424 (1987).
- [10] Z. S. She and E. Leveque, *Phys. Rev. Lett.* **72**, 336 (1994).
- [11] R. Benzi, S. Ciliberto, C. Baudet, and G. R. Chavarria, *Physica D* **80**, 385 (1995).
- [12] S. Grossmann, D. Loshe, V. L'vov, and I. Procaccia, *Phys. Rev. Lett.* **73**, 432 (1994); S. I. Vainshtein and K. R. Sreenivasan, *ibid.* **73**, 3085 (1994).
- [13] L. P. Kadanoff, *Phys. Today* **48**(9), 11 (1995).
- [14] R. H. Kraichnan, *Proc. R. Soc. London, Ser. A* **434**, 65 (1991).
- [15] J. Qian, *J. Phys. A* **31**, 3193 (1998).